International Journal of Current Engineering and Technology
E-ISSN 2277 – 4106, P-ISSN 2347 - 5161

Available at http://inpressco.com/category/ijcet

Research Article

Synthesis, Characterization and DC Conduction Mechanism in Inverse Spinel Compound (Mg_2TiO_4)

Alok Kumar Singh[Á*], Anju Dhillon[B], T.D.Senguttuvan[Ć] and Azher M. Siddiqui[Á]

[Á]Department of Physics, Jamia Millia Islamia (Central University), New Delhi-25, India
[B]Department of Applied Science, Maharaja Surajmal Institute of Technology, GGSIP University, New Delhi-58, India
[Ć]National Physical Laboratory, New Delhi, India

Accepted 25 February 2014, Available online 28 February 2014, **Vol.4, No.1 (February 2014)**

Abstract

Magnesium Ortho Titanate (Mg_2TiO_4) has been synthesized by solid state reaction technique and characterized by X-ray diffraction (XRD), Scanning Electron Microscopy (SEM) and dc conductivity. Powder x-ray diffraction analysis indicates single phase nature cubic structure with space group Fd3m. The surface morphology of the sample is investigated by Scanning Electron Microscopy (SEM) which indicates the occurrence of curious cubical growth characteristics resembling a spiral like feature which have emanated from screw dislocations. The dc conductivity of the sample was measured over the range of temperature 77-300 K. The measured room temperature conductivity of the sample is 6.52 $\times 10^{-7}$ Ohm^{-1} cm^{-1}. An effort has been made to explain the conduction mechanism in this sample in terms of the so called Mott's variable range hopping model. The hopping conduction parameters such as the characteristic temperature (T_0), localization length (α), hopping distance (R), activation energy (ΔE), average hopping energy (W) and density of states at the Fermi level (N (E_F)) have been worked out.

Keywords: *X-ray diffraction pattern, Scanning Electron Microscopy, Calcination, Sintering, Defects, Grain size, Electrical conductivity, Spinels, Hopping model, Screw dislocation.*

Introduction

Spinel compounds are being extensively studied for their applications in dew sensors, pigments for protective coatings etc. (P. K. Roy *et al*, 2007; C. P. Poole *et al*, 1982; E. J. W. Verwey *et al*, 1936). These materials find wide industrial applications in dew sensors, pigments for protective coatings and principally for their dielectric properties in chip capacitors, high frequency capacitors and temperature compensating capacitors and in the composition of binders by increasing the flexural strength (M. J. M. Lope *et al*, 1992). The properties of these materials are highly dependent on the structural disorder arising from synthesis procedure and sintering temperature (H. Hohl *et al*, 1996). They exhibit a rich diversity in morphology because of their highly crystalline nature. The electrical property varies from an insulating to a conducting regime (M. Okutan *et al*, 2005; W. A. Badawy *et al*, 1990) hence resulting in a wide range of conductivities. Various charge transport mechanisms have been proposed depending on the conductivity behavior of ceramics with various parameters such as temperature, pressure and doping (W. K. Park *et al*, 2003; J. H. Cho *et al*, 2004; R. C. da Silva *et al*, 2002; H. Bottger *et al*, 1995; R. Mansfield *et al*, 1991; A. Hausmann *et al*, 1972). Detailed investigations on inverse spinels have recently started.

The compounds Mg_2TiO_4 refers to the inverse (reversible) spinel type structure (Space group Fd3m and Z=8) with structural formula $(Mg)^{2+}[Mg^{2+}Ti^{4+}]O_4$ (N. Stubicar *et al*, 2004; B. D. Lee *et al*, 2003; A. Golubovic *et al*, 2011). Their valency distribution has been described elsewhere (A. K. Singh *et al*, 2013).

In this study, we report the synthesis, X-ray diffraction, surface morphology and conductivity behavior of the inverse spinel compound, Mg_2TiO_4. The room temperature conductivity of the sample has been calculated several times by various authors, but the conduction mechanism has not been analyzed yet to the best of our knowledge.

Growth mechanism

Each crystal system tends to give a unique defect structure; such defects are presented during the crystal growth stage. The application of any crystal relies only upon the functionality of these materials for which it is essential to control the defects and the crystal size (B. Subotic *et al*, 2003).

The growth mechanism in case of spinal structures is unfavorable as a minor adjustment in the occupying of tetrahedral or octahedral sites results in either a spinel type

*Corresponding author: **Alok Kumar Singh's** phone +91-11-2698461, Fax: +91-11-26981753

or inverse spinel type structure. The consequential pattern is a curious spiral like structure; each grain or column grows by accumulation molecules to a spirally expanding ramp on the top surface of the grain (M. Hawley *et al*, 1991) as suggested by Frank (F. C. Frank *et al*, 1949) in the classical curved growth mechanism. These dislocations will create steps in the surface, obviating the inevitability for 2D nucleation.

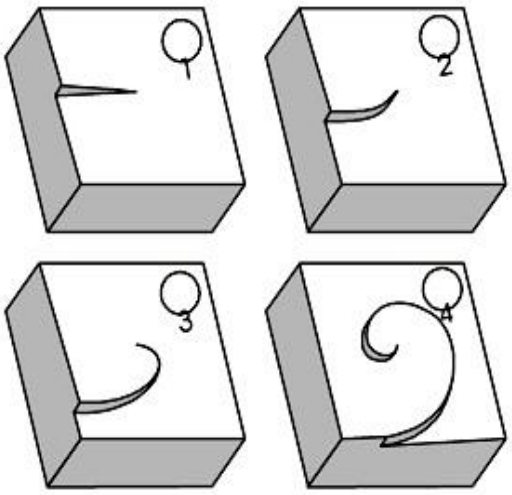

Fig.1. Crystal growth mechanism by screw dislocation

Fig.1 shows a schematic diagram on the concern and the fruition of curved development. The spiral growth mechanism was developed theoretically by Burton et al. (W. K. Burton *et al*, 1951) and observed experimentally for the first time by Verma & Krishna (A. R. Verma *et al*, 1996). The theory of crystal development by spiral dislocation was further refined by Burton, Cabrera and Frank (W. K. Burton *et al*, 1951) giving rise to what is acknowledged as BCF theory.

Experimental

Polycrystalline sample of inverse spinel Mg_2TiO_4 was synthesized by solid state reaction technique, with composition $Mg_{2-x}Ti_{1-x}O_4$. Here x is referred to as inversion parameter. The stoichiometric amount of $Mg(NO_3)_2.6H_2O$ (98.5 %) and TiO_2 (Rutile, 99.5 %), powders were mixed thoroughly and pre-calcined for 12 h at 1000º C. The pre-calcined material was again ground and calcinated at 1250º C for 24 h. Finally the sample was ground to fine powder, pressed to pellet form and sintered at 1300º C for 72 h and at the end of heat treatment the sample was allowed to cool slowly at room temperature (A. K. Singh *et al*, 2013). The X-ray powder diffraction patterns after sintering were obtained using a Philips PW-1050 diffractometer with λ Cu-Kα irradiation and a step/time scan mode of 0.02 degrees per second and data was analyzed by Powder X software (C. Dong *et al*, 1999). Surface morphology was analyzed by Surface Electron Microscopy (SEM) model LEO (440). The dc conductivity studies in the temperature range 77–300 K were carried out by a two probe method using Keithley's 610 C electrometer and 236 source meter unit (SMU).

Results and Discussion

X-ray diffraction

The XRD pattern of Mg_2TiO_4 at room temperature is shown in fig. 2 exhibits single phase nature (M. J. M. Lope et al, 1992).

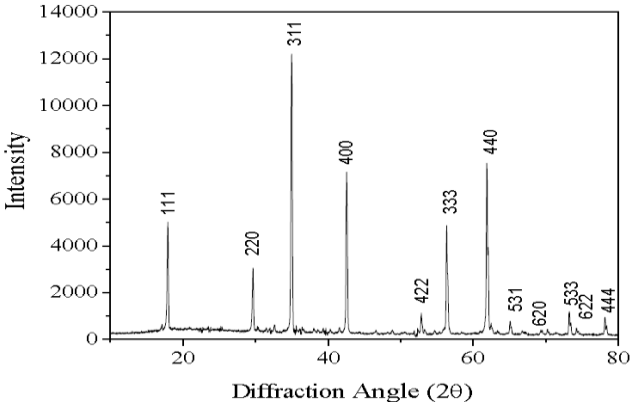

Fig. 2 X-ray diffraction pattern of single phase Mg_2TiO

XRD spectrum was indexed using Powder X software from where it can be inferred that the system exhibits cubic spinel structure with space group Fd3m (A. K. Singh *et al*, 2011; G. Kimmel *et al*, 2000) and lattice constant 8.456 Å.

Scanning Electron Microscopy

Depending upon the annealing duration the presence of cubic structures of various sizes (1-2 μm) are revealed by SEM images. The shape of these compounds is directly dependent on the relative order of surface energy.

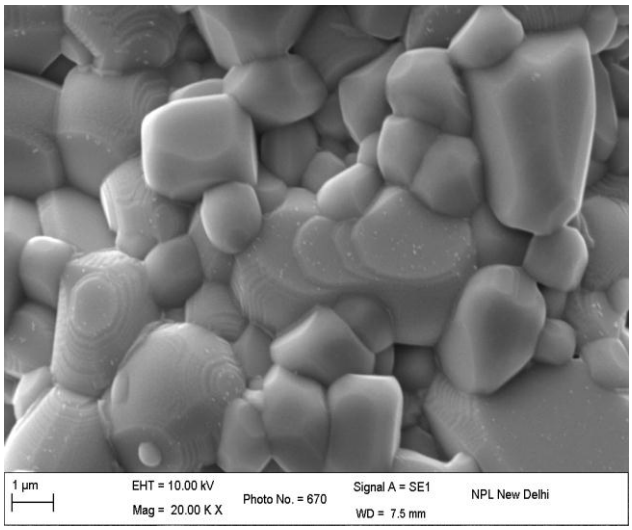

Fig 3 a

Fig. 3 (a, b) in SEM micrograph reveals curious growth characteristics; it also clearly demonstrates the nucleation of new step on an atomically smooth surface. We observe closed spiral like loops in assorted forms. Fig. 3 (a) is the

SEM image of Mg_2TiO_4 which exhibits curious microstructural characteristics in the form of a myriad spiral like growth features. These can be classified as either columnar or tangential (A. K. Singh *et al*, 2013). Fig. 3 (b) is the magnified image of the sample with size 200 nm, which shows cubical growth as well as screw dislocation (F. C. Frank *et al*, 1949; W. K. Burton *et al*, 1951; A. R. Verma *et al*, 1996; A. K. Singh *et al*, 2013; C. Dong *et al*, 1999; A. K. Singh *et al*, 2011; G. Kimmel *et al*, 2000; J. Zabicky *et al*, 2009).

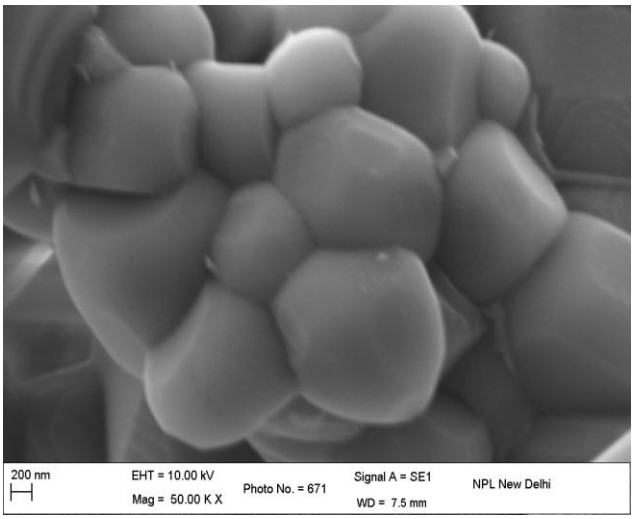

Fig 3 b

Fig.3 Cubical structure of the inverse spinel Mg_2TiO_4 shown by SEM

Possible mechanism for the generation of spiral like growth features of Mg_2TiO_4

A careful analysis of these samples shows cubical spiral features which are mediated through screw dislocation (F. C. Frank *et al*, 1949). The introduction mechanism of dislocation in these high temperature materials is not yet understood fully. The ascendancy of the density of dislocations is important for high current device applications. One important condition of the spiral like growth is the sintering temperature as well as the estimated temperature during the solid state reaction technique. It was predicted that the growth is totally cubic in structure. It may be possible that when the two growth fronts corresponding to $Mg(NO_3)_2.6H_2O$ and TiO_2 would develop sufficiently and meet each other over an earlier grown structure, a screw dislocation would form due to incoherent meeting. That is normal at this stage of development. It is not possible to pin-point and it is not possible at this point to a certain whether interacting and interlaced circular and cubic spiral features or single cubic spiral features or spirals containing inclusion/platelet like features or even square spiral features truncated at the corners gives to them specific structure. Nevertheless, regardless of the details of the mechanism, it is certain that the material after the initial developments in the shape of crystallites develops further through spiral growth mechanism.

Electrical conductivity

In order to determine the mechanism of conduction in spinels, usually the temperature dependence of the electrical conductivity is studied over the wide range of temperature (W. A. Badawy *et al*, 1990; H. M. El-Mallah *et al*, 2004; R. C. Kambale *et al*, 2010; H. M. El-Mallah *et al*, 2007; D. H. Lee *et al*, 1998; K. Yagasaki *et al*, 2002; I. Khan *et al*, 2011).The conductivity can be assumed to consist of two parts, namely σ_B and σ_H, such that the total DC conductivity $\sigma_{dc} = \sigma_B + \sigma_H$. σ_B can be reported by the mechanism in the band conduction model for the high temperature, whereas σ_H is a contribution due to charge transport at lower temperatures.

The total conductivity of the ceramic was determined as the summation of the contributions from the two different conduction mechanisms. The conductivity is expressed by

$$\sigma\,(T) = \sigma_1 \exp(-\Delta E/k_B T) + \sigma_o \exp[-(T_o/T)^{-1/4}] \qquad (1)$$

It is evaluated that at below 300 K, the charge transfer mechanism between localized states can be explained using Variable Range Hopping (VRH) model. The hopping conduction is associated with electron jumping from an occupied site to empty ones. The empty sites can be fulfilled at low temperatures. Hopping conductivity is governed by the hopping probability between occupied and unoccupied sites. At high temperatures, the hopping probability is dominated by the random spatial distribution of the atomic sites.

At higher temperatures, conductivity mechanism is mainly determined by hopping of carrier thermally activated into the band tails as mono-energetic trap state becomes thermodynamically accessible at higher temperatures. In fact, the variable hopping regime dominating at lower temperature region should change to the constant range regime with increasing temperature because the hopping distance will reach its minimum possible value when the carriers jump between the nearest neighbor sites (N. F. Mott *et al*, 1979).

The ceramic indicates the typical behavior of a semiconductor as its electrical conductivity increases with increasing temperature (D. H. Lee *et al*, 1998). Similar behavior has been observed for the Mg_2TiO_4 and the variation of dc conductivity as a function of 1000/T in the temperature range 77-300K is shown in Fig. 4.

For the lower temperatures, the conductivity results have been examined in the light of Mott's variable range hopping (VRH) model (N. F. Mott *et al*, 1979; Z. Yang *et al*, 2002; M. Ziese *et al*, 1998; R. M. Kusters *et al*, 1989; G. J. Snyder *et al*, 1996; C. Ang *et al*, 1998). In this model, the dc conductivity shows the temperature dependence of type T^{-n} where n = 1/1+d, and d is the dimensionality. Therefore, Mott's model suggests n=1/2 for one dimensional hopping, n = 1/3 for two dimensional hopping and n =1/4 for three dimensional hopping. From Figs. 4 (b), (c) & (d) the linear regression on the data points in entire temperature range of measurement gives the maximum linearity factor and hence best fit for $T^{-1/4}$ for the sample. So, 3D VRH seems to be a dominant charge transport mechanism.

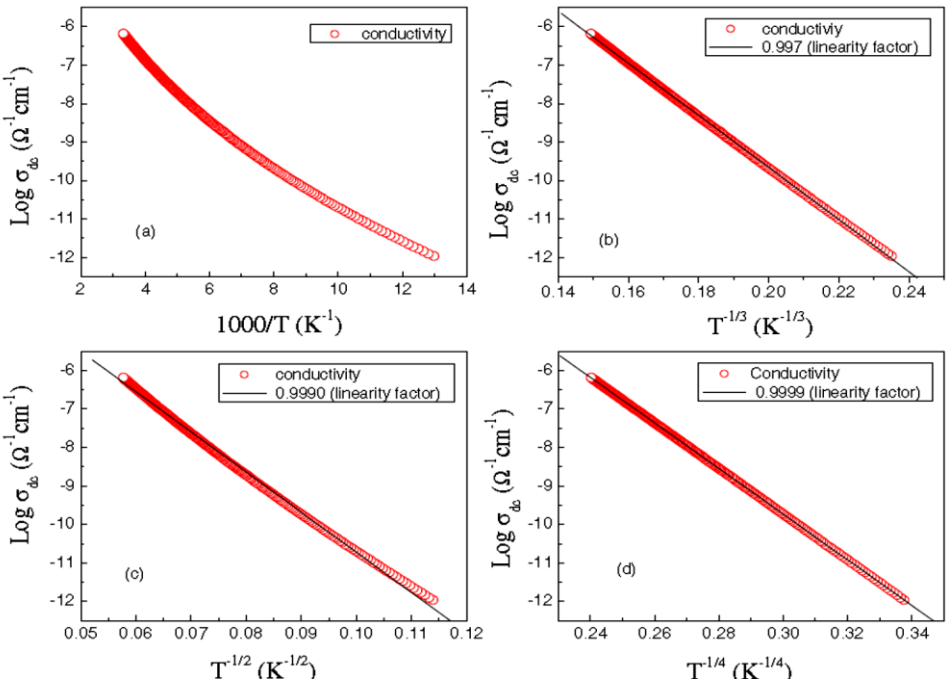

Fig.4 Variation in dc conductivity as a function of (a) 1000/T, (b) $T^{-1/2}$, (c) $T^{-1/3}$, and (d) $T^{-1/4}$ in the temperature range of 77–300 K for Mg_2TiO_4

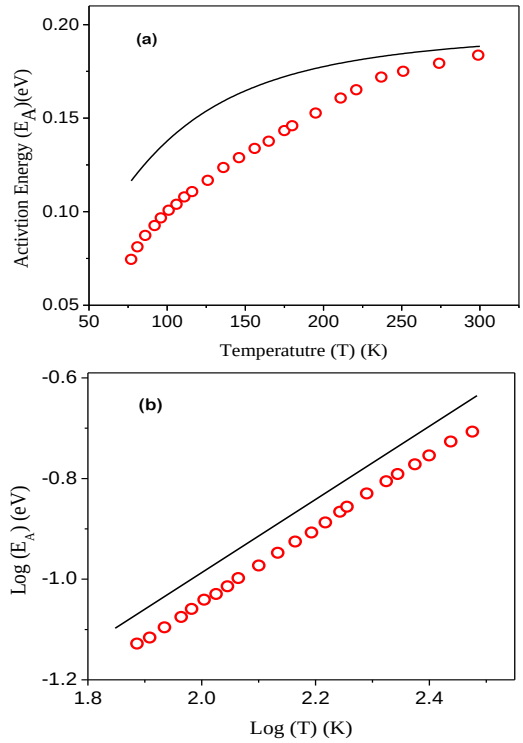

Fig.5 Plot of (a) activation energy E_A vs. temperature and (b) log activation energy vs. log temperature of Mg_2TiO_4.

Fig. 5(a) and 5(b) show the temperature dependence of activation energy, calculated from Fig. 4(a). The values of the activation energy along with that of dc conductivity at 300 K and 77 K are given in Table 1. The observed temperature dependence of activation energy rules out band conduction at the low temperature.

$$E_A = -\, d \ln\sigma / dT \qquad (2)$$

Table 1 Dc conductivity (σ_{dc}) and activation energy (E_A) at 77K & 300K of Qandilite (Mg_2TiO_4)

Sample	Conductivity σ_{dc} ($\Omega^{-1}cm^{-1}$)		E_A (eV)	
	77K	300 K	77 K	300 K
Mg_2TiO_4	1.07×10^{-12}	6.52×10^{-7}	0.074	0.183

Mott (N. F. Mott *et al*, 1979) has suggested that hopping may take place preferentially beyond nearest neighbors. The variable range hopping conductivity predicted by Mott and Davis, (N. F. Mott *et al*, 1979) is of the form

$$\sigma_H = \sigma_o \exp\,[-(T_0/T)^n] \qquad (3)$$

where T_0 and σ_0 are constants and can be expressed as.

$$T_o = \lambda\alpha^3/k_B\,N(E_F) \qquad (4)$$

and

$$\sigma_o = e^2R^2\vartheta_o N(E_F) \qquad (5)$$

where T_0 is the characteristic temperature, λ is a dimensionless constant (W. A. Badawy *et al*, 1990; D. K. Paul *et al*, 1973) and is assumed to be either 18 or 21 (W. A. Badawy *et al*, 1990; N. F. Mott *et al*, 1979; F. Yakuphanoglu *et al*, 2004), α is the coefficient of exponential decay of the localized states involved in hopping process. A reasonable estimates for α is $\alpha=1/r_P$ where r_P is equivalent to the bond length in this system, i.e, 2 Å, as determined from the refinements of neutron and synchrotron diffraction patterns (M. P. Sharma *et al*, 2011; K. Suri *et al*, 2003; A. Banerjee *et al*, 2003; A. I. Ali *et al*, 2007; B. A. Wechsler *et al*, 1989; G. Kimmel *et al*, 2004). K_B is the Boltzmann's constant, N (E_F) is the density of states at the Fermi level, e is the electronic charge, σ_0 is

the conductivity at infinite temperatures, υ_0 is the phonon frequency (~1013Hz) and can be obtained from Debye's temperature θ_D, (R. Singh *et al*, 1993) and R is the hopping distance between the two situations.

The plot in the temperature region where Eq. (3) is valid should give activation energy as per Eq. (2) and can be correlated to the parameters of Eq. (3) by the following equation

$$E_A = nk_BT_o(T_o/T)^{n-1} \quad (6)$$

It is evident from Eq.(6) that a plot of $\log E_A$ versus log T should yield a straight line of slope (n-1). The solid line corresponding to n=1/4 is shown in Fig. 5(b). It can be ascertained that the slope of the solid line is nearly parallel to obtain log activation energy data versus log T. This further indicates that three dimensional variable range hopping is dominant in the present case.

The temperature dependent activation energy can also be qualitatively explained if polaronic hopping is considered (H. M. El-Mallah *et al*, 2007; D. H. Lee *et al*, 1998; O. Bidauit *et al*, 1995; K. A. Muller *et al*, 1979). According to Holstein (T. Holstein *et al*, 1959), for orders material having polaronic hopping conduction, multi-phonon processes are involved. These are gradually replaced at lower temperatures by the processes in which the only contribution to the jump frequency of the polaron is due to single optical phonon absorption or emission. The variation of activation energy for such a procedure is given by

$$\frac{E_{A'}}{E_A} = \frac{\left[tanh\left(\frac{\hbar\omega_0}{4k_BT}\right)\right]}{\left(\frac{\hbar\omega_0}{4k_BT}\right)} \quad (7)$$

where E_A is the room temperature activation energy, $\omega_0 = 2\pi\upsilon_0$, $\hbar = h/2\pi$, $E_{A'}$ is the activation energy for different temperatures. As a representative result, theoretical plot for $E_{A'}$ from Eq. (7) has been shown as solid line in Fig. 5(a) for the sample. It can be seen that the Polaronic hopping conduction can give temperature-independent activation energy, where multi-phonon process dominates. Nevertheless, the temperature dependent activation energy rules out the above possibility, confirming the existence of Polaronic conduction through VRH where single photon processes are involved in the sample.

Furthermore, for Mott's theory to be applicable for the evaluation of hopping parameters a good fit of conductivity Vs temperature data is essential (R. Singh *et al*, 1996). The hopping conductivity is given for the spinel in Fig. 4. The other hopping parameters which are hopping distance (R) and the average hopping energy (W) can be defined by the following relations:

$$R = [9/8\pi\alpha k_BTN(E_F)]^{1/4} \quad (8)$$

and

$$W = [3/4\pi R^3N(E_F)] \quad (9)$$

Mott's parameters T_0, R, W and $N(E_F)$ are given in Table2

Table 2 Calculated Mott's Parameters: characteristic temperature (T_0), density of states at Fermi level ($N(E_F)$), average hopping distance (R) and average hopping energy (W), of Qandilite (Mg_2TiO_4).

Sample	T_0 (K)	$N(E_F)$(cm^{-3} eV^{-1})	R (cm)	W(eV)	αR
Mg_2TiO_4	$1.24x10^7$	2.53×10^{21}	$10.22x\ 10^{-8}$	0.0881	5.11

The estimated values are consistent with the Mott's requirement that αR >> 1 and W >> k_BT for hopping to distant sites. The value of $N(E_F)$ is reasonable ($2.53x10^{21}$ cm^{-3} eV^{-1}), much below the Avogadro Number in the given range. From the above observations and subsequent calculations, it can be inferred that at lower temperatures the 3D VRH is the basic transport mechanism, whereas at higher temperatures the hopping probability is dominated by the random spatial distribution of the atomic sites.

Conclusions

Magnesium Ortho Titanate (Mg_2TiO_4) has been prepared by conventional solid state reaction technique on sintering at 1300° C for 72 hours. The XRD pattern of Mg_2TiO_4 shows its single phase nature exhibiting cubic spinel structure with space group Fd3m and lattice constant 8.456 Å. SEM images of the sample show the curious microstructural characteristics in the form of myriad spiral like growth features. The charge transport mechanism has been well explained by 3D Mott's variable range hopping model and the density of states is found to be $N(E_F) = 2.53 \times 10^{21}$ cm^{-3} eV^{-1} which is well within the range.

Acknowledgments

The authors are grateful to National Physical Laboratory, New Delhi, India for the experimental assistance and UGC for financial support.

References

P. K. Roy, J. Bera (2007), Enhancement of the magnetic properties of Ni–Cu–Zn ferrites with the substitution of a small fraction of lanthanum for iron, *Mater. Res. Bull.*, 42, 77-83

C. P. Poole, H. A. Farach (1982), Magnetic phase diagram of spinel spin-glasses, *Z. Phys. B.*, 47, 55-57.

E. J. W. Verwey, J. H. deBoer (1936), Cation arrangement in a few oxides with crystal structures of the spinel type, *Rec. Trav. Chim. Pays. Bas*., 55, 531-540

M. J. M. Lope, M. P. B. Pena and M. E. G. Clavel (1992), The composition of magnesium titanates as a function of the synthesis methods, *Therm. Acta.*, 194, 247-252.

H. Hohl, C. Kloc, E. Bucher (1996), Electrical and Magnetic Properties of Spinel Solid Solutions $Mg_{2-x}Ti_{1+x}O_4$; $0 \leq x \leq 1$, *J. of Solid State Chem.*, 125, 216-223.

M. Okutan, H. I. Bakan, K. Korkmaz, F. yakuphanoglu (2005), Variable range hopping conduction and microstructure properties of semiconducting Co-doped TiO_2**,** *Phys. B.*, 355, 176-181.

W. A. Badawy, R. S. Momtaz, E. M. Elgiar (1990), Solid State Characteristics of Indium-Incorporated Titanium Dioxide (TiO_2), *Thin Films, Phys. Stat. Sol. (A).*, 118, 197-202

W. K. Park, R. J. Ortega-Hertogs, J. S. Moodera, A. Punnoose, M. S. Seehra (2003), Semiconducting and ferromagnetic

behavior of sputtered Co-doped TiO_2 thin films above room temperature, *J. Appl. Phys*., 91 (10), 8093-8096

J. H. Cho, B. Y. Kim, H. D. Kim, S. I. Woo, S. H. Moon, J. P. Kim, C. R. Cho, Y. G. Joh, E. C. Kim, D. H. Kim (2004), Enhance ferromagnetism in Co-doped TiO_2 powders, *Phys. Status solidi B*, 241 (7), 1537-1540.

R. C. da Silva, E. Alves, M. M. Cruz (2002), Conductivity behaviour of Cr implanted TiO_2, *Nucl. Instr. Meth. B.*, 191, 158-162.

H. Bottger, V. V. Bryksin (1985), Hopping Conduction in solids ~ VCH, Verlagsgesellschaft, *Weinheim, Germany.*

R. Mansfield, in M. Pollak, B. I. Shklovskii (Eds.)(1991), .Hopping transport in solids, *North Holland, Amsterdam*

A. Hausmann, W. Teuerle, Konzentration und Beweglichkeit von (1972), Elektronen in Zinkoxidkristallen mit Indium-Dotierung, *Z. Phys. A*, 257, 299-309.

N. Stubicar, A. Tonejc, M. Stubicar (2004), Microstructural evolution of some MgO–TiO_2 and MgO–Al_2O_3 powder mixtures during high-energy ball milling and post-annealing studied by X-ray diffraction, *J. Alloys compd.*, 370, 296-301.

B. D Lee, K. H Yoon, E. S Kim, T. H Kim (2003), Microwave Dielectric properties of $CaTiO_3$ and $MgTiO_3$ Thin films, *Jpn. J. Appl. Phys.*, 42, 6158-6161.

A. Golubovic, M. Radovic (2011), The growth of Mg_2TiO_4 single crystals using a four-mirror furnace, *J. Serb. Chem. Soc.*, 76 (11), 1561-1566.

A. K. Singh, A. Dhillon, T. D. Senguttuvan, A. M. Siddiqui (2013), Study of curious spiral like features in inverse spinel compound (Mg_2TiO_4), *Int. J. Adv. Res. Sci. Technol*., 2, 63-66.

B. Subotic, J. Bronic (2003), Handbook of Zeolite Science and Technology, *Marcel Dekker, New York,* pp. 1184.

M. Hawley, I. D. Raistrick, J. C. Berry, R. J. Houlton (1991), Growth mechanism of sputtered films of $YBa_2Cu_3O_7$ studied by scanning tunneling microscopy, *Science*, 251, 1587-1589.

F.C. Frank (1949), Discuss, The influence of dislocation on crystal growth, *Faraday Soc.*, 5, 48-54.

W. K. Burton, N. Canbera, F. C. Frank (1951), The growth of crystals and the equilibrium structure of their surfaces, *Philos Trans. R. Soc., (*A 243), 299-358.

A.R. Verma , P. Krishna (1996), Polymorphism and polytypism in Crystal, *John Wiley & sons Inc. New York*

C. Dong (1999), Powder X: Windows-95-based program for powder X-ray diffraction data processing, *J. Appl. Cryst.*, 32, 838-839.

M. J. M. Lope, M. P. B. Pena and M. E. G. Clavel (1992), The composition of magnesium titanates as a function of the synthesis methods, *Therm. Acta.*, 194, 247-252.

A. K. Singh, R. Kumar, T. D. Senguttuvan, and A. M. Siddiqui (2011), Synthesis and structural analysis of Al-doped qandilite (Mg_2TiO_4), *AIP Conf. Proc.*, 1393, 235-236

G. Kimmel, J. Zabicky (2000), International centre for diffraction data 2000, *Advances in X- ray Analysis*, 42, 238-244.

J. Zabicky, G. Kimmel, E. Goncharov, F. Guirado (2009), *Z. Kristallogr. Suppl.*, 30, 347-352.

H. M. El-Mallah (2004), D. C. conduction mechanisms of certain perovskite ceramics, *J. Mater. Sci.*, 39, 1711-1715

R. C. Kambale, N. R. Adhate, B. K. Chougule, Y. D. Kolekar (2010), Magnetic and dielectric properties of mixed spinel Ni–Zn ferrites synthesized by citrate–nitrate combustion method, *J. Alloys Compds.*, 491, 372-377

H. M. El-Mallah, M. S. Aziz (2007), Structural and Conduction Mechanisms Studies in Strontium Lanthanum Titanate Perovskite, SLT Ceramic, *Egypt. J. Solids*, 30: 19-29

D. H. Lee, H. S. Kim, C. H. Yo, K. Ahn, K. H. Kim (1998), The magnetic properties and electrical conduction mechanism of $Co_{1-x}Mn_xFe_2O_4$ spinel, *Mater. Chem. & Phys.*, 57, 169-172

K. Yagasaki, T. Nakama, M. Hedo, K. Uchima, Y. Shimoji, N. Matsumoto, S. Nagata, H. Okada, H. Fuji, A. T. Burkov (2002), *J. Phys. & chem. Solids*, 63, 1051-1054

I. Khan, M. Zulfequar (2011), Structural and Electrical Characterization of Sintered Silicon Nitride Ceramic, *Mater. Sci. & App.*, 2, 738-747.

N. F. Mott and E. A. Davis (1979), Electronic Processes in Non-crystalline Materials 2nd ed *(London: Oxford University Press).*

Z. Yang, S. Tan, Y. Zhang (2002), Colossal magnetoresistance effect in the inverse spinel $FeCr_{2-x}Ga_xS_4$, *Phys. Rev. B.*, 65, 1844041-1844047.

M. Ziese, C. Srinitiwarawong (1998), Polaronic effects on the resistivity of manganite thin films, *Phys. Rev. B.*, 58, 11519-115125.

R. M. Kusters, J. Singleton, D. A. Keen, R. McGreevy, W. Hayes (1989), Magnetoresistance measurements on the magnetic semiconductor $Nd_{0.5}Pb_{0.5}MnO_3$, *Physica B.*, 155, 362-365

G. J. Snyder, R. Hiskes, S. Dicarolis, M. R. Beasley, T. H. Geballe (1996), Intrinsic electrical transport and magnetic properties of $La_{0.67}Ca_{0.33}MnO_3$ and $La_{0.67}Sr_{0.33}MnO_3$ MOCVD thin films and bulk material, *Phys. Rev. B.*, 53, 14434-14444.

C. Ang, J. R. Jurado, Z. Yu, M. T. Colomer, J. R. Frade, J. L. Baptista (1998), Variable-range-hopping conduction and dielectric relaxation in disordered $Sr_{0.97}(Ti_{1-x}Fe_x)O_{3-\delta}$, *Phys. Rev. B.*, 57, 11858-11861.

D. K. Paul, and S. S. Mitra (1973), Evaluation of Mott's Parameters for Hopping Conduction in Amorphous Ge, Si, and Se-Si, *Phys Rev. Lett.*, 31, 1000-1003.
F. Yakuphanoglu, M. Aydin, N. Arsu, M. Sekerci (2004), A small molecule organic semiconductor, *Semiconductors*, 38, 468-471.

M. P. Sharma, A. Krishnamurthy, B. K. Srivastava (2011), Transport Properties of the Layer Manganite $La_{1.5}Ca_{1.5}Mn_{2-x}Fe_xO_7$, *World J. Cond. Matt. Phys.*, 1, 153-156.

K. Suri, S. Annapoorni, R. P. Tandon (2003), AC conduction in nano-composites of polypyrrole, *J. of Non-Cryst. Solids*, 332, 279–285.

A. Banerjee, S. Bhattacharya, S. Mollah, H. Sakata, H. D. Yang, B. K. Chaudhuri (2003), Evidence for the immobile bipolaron formation in the paramagnetic state of the magneto-resistive manganites**,** *Phys. Rev. B.*, 68, 186401-186405.

A. I. Ali, A. Hassen, Bongju Kim, Y. Wu, B. G. Kim, S. H. Park (2007), Magnetic Phase Transition and Variable Range Hopping Conduction of $Y_{1-x}Sr_xCoO_3$-\delta, *J. Korean Phys. Soc.*, 51, 1736-1742.

B. A. Wechsler, R. B. Von Dreele (1989), Structure refinements of Mg_2TiO_4, $MgTiO_3$ and $MgTi_2O_5$ by time-of-flight neutron powder diffraction, *Acta Cryst.*, B45, 542-549.

G. Kimmel, J. W. Richardson, R. Xu, P. Ari-Gur, E. Goncharov, J. Zabicky (2004), International centre for diffraction data 2004, *Advances in X- ray Analysis*, 47, 261-266.

R. Singh, R. P. Tandon, S. Chandra (1993), Evidence of small-polaron formation in polypyrrole, *J. Phys: Condens. Matter*, 5, 1313-1316.

O. Bidauit, M. Maglione, M. Actis, M. Kchikech, B. Salce (1995), Polaronic relaxation in perovskites, *Phys. Rev. B.*, 52, 4191-4197.

K. A. Muller, H. Kleemann, J. G. Bednorz (1979), $SrTiO_3$: An intrinsic quantum paraelectric below 4 K, *Phys. Rev. B.*, 19, 3593-3602.

T. Holstein (1959), Studies of polaron motion: Part II. The "small" polaron, *Ann. Phys.*, 8, 343-389.

R. Singh and A. K. Narula (1996), Correlation between dielectric-relaxation and dc electrical-conduction in polypyrrole family of polymers, *Synth. Met.*, 82, 245-249.